Pharm Res (2015) 32:1804–1816
DOI 10.1007/s11095-014-1577-y

RESEARCH PAPER

The Secondary Drying and the Fate of Organic Solvents for Spray Dried Dispersion Drug Product

Daniel S. Hsieh • Hongfei Yue • Sarah J. Nicholson • Daniel Roberts • Richard Schild • John F. Gamble • Mark Lindrud

Received: 25 June 2014 / Accepted: 13 November 2014 / Published online: 17 December 2014

ABSTRACT

Purpose To understand the mechanisms of secondary drying of spray-dried dispersion (SDD) drug product and establish a model to describe the fate of organic solvents in such a product.

Methods The experimental approach includes characterization of the SDD particles, drying studies of SDD using an integrated weighing balance and mass spectrometer, and the subsequent generation of the drying curve. The theoretical approach includes the establishment of a Fickian diffusion model.

Results The kinetics of solvent removal during secondary drying from the lab scale to a bench scale follows Fickian diffusion model. Excellent agreement is obtained between the experimental data and the prediction from the modeling.

Conclusions The diffusion process is dependent upon temperature. The key to a successful scale up of the secondary drying is to control the drying temperature. The fate of primary solvents including methanol and acetone, and their potential impurity such as benzene can be described by the Fickian diffusion model. A mathematical relationship based upon the ratio of diffusion coefficient was established to predict the benzene concentration from the fate of the primary solvent during the secondary drying process.

KEY WORDS amorphous · Fickian diffusion · modeling · secondary drying · spray dried dispersion

ABBREVIATIONS

API	Active pharmaceutical ingredient
D	Diffusion coefficient
DSC	Differential scanning calorimetry
GC	Gas chromatography
HPMCAS	Hydroxypropylmethylcellulose (hypromellose) acetate succinate
ICH	International conference of harmonisation
MS	Mass spectroscopy
PSD	Particle size distribution
PVP K30	Polyvinylpyrrolidone K30
PXRD	Powder x-ray diffraction
SDD	Spray dried dispersion
SEM	Scanning electron microscope
T_g	Glass transition temperature
α_{AB}	Relative diffusion rate of solvent A with respect to solvent B
β	Diffusion parameter

INTRODUCTION

Spray Dried Dispersion (SDD) technology has been increasingly utilized for drugs with low aqueous solubility to enhance the solubility and bioavailability of drug product (1–4). In this technology, as shown in Fig. 1, a solution of Active Pharmaceutical Ingredient (API) and stabilizing polymer in organic solvent is fed to an atomizing nozzle in a spray dryer unit to generate small liquid droplets which are immediately dried in the drying chamber with hot nitrogen. After the drying chamber, the solid particles are separated from the gas phase and collected at the bottom of the cyclone. Due to the presence of polymer and a very short residence time, normally less than

D. S. Hsieh (✉) • D. Roberts
Drug Product Science & Technology, Bristol-Myers Squibb Company, One Squibb Drive, New Brunswick, New Jersey 08903, USA
e-mail: daniel.hsieh@bms.com

H. Yue
Analytical and Bioanalytical Development, Bristol-Myers Squibb Company, One Squibb Drive, New Brunswick, New Jersey 08903, USA

S. J. Nicholson • J. F. Gamble
Drug Product Science & Technology, Bristol-Myers Squibb Company, Reeds Lane, Moreton, Merseyside CH46 1QW, UK

R. Schild • M. Lindrud
Chemical Development, Bristol-Myers Squibb Company, One Squibb Drive, New Brunswick, NJ 08903, USA

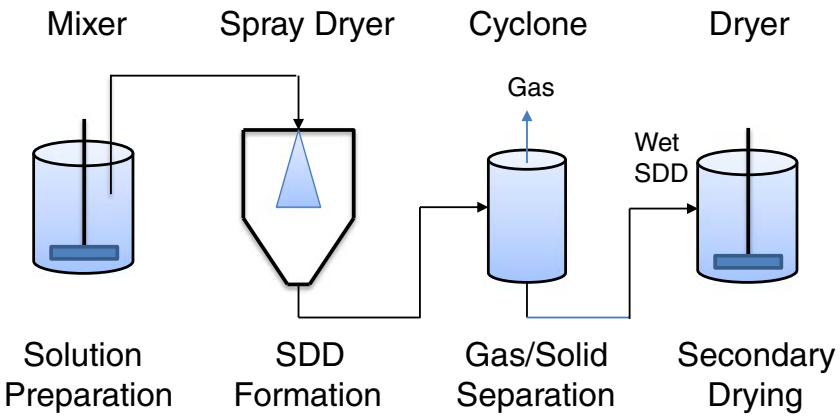

Fig. 1 Schematic diagram of spray-dried dispersion process.

30 s (5) in the drying chamber, the organic solvent cannot be fully removed in a typical spray dryer unit. Hence, a secondary drying process is needed to further reduce the residual organic solvents to a concentration below the ICH guideline (6). The solvents of interest in this study are acetone and methanol (which are controlled to meet ICHQ3C (R5) requirements) and benzene (an ICH Class 1 solvent) which could be present at ppm levels as a by-product of the production of acetone and methanol. To optimize the process systematically, it is critical to understand the drying mechanism. In this study, first, the fundamental drying mechanisms are elucidated. Second, a mathematical mass transfer model is established on the basis of the drying mechanism and the characteristics of the solid particles. Third, this mass transfer model is verified with lab scale experiments as well as large scale batches. Finally, this established model is used to develop the secondary drying protocol and to predict the fate of organic solvents and solvent-related impurity such as benzene (7) in SDD products.

The execution of the above-mentioned studies includes both experimental and theoretical approaches, including the generation of the drying curve from a weighing balance, the characterization of the materials, the identification of evaporation and Fickian diffusion patterns from the drying curve and the establishment of a mathematical model from the understanding of the morphology of the SDD product. Two SDD systems are included in this study. The first one is Compound A with polyvinylpyrrolidone K30 (PVP K30) as the stabilizing polymer to understand the drying mechanisms and to establish the secondary drying model. The second is hydroxypropylmethylcellulose (hypromellose) acetate succinate (HMPCAS) alone (i.e. without API) to study the fate of primary solvents as well as benzene. The drying model established from the first SDD system is used to estimate how much and how fast the solvents, especially the benzene impurity, can be removed from the SDD product via secondary drying.

Although diffusion-based drying kinetics of polymers has been widely studied (8), this work is focusing on the mechanistic understanding of secondary drying of polymer-stabilized amorphous SDD of API. The methodology developed in this study can be applied broadly to the drying processes of a variety of SDDs to predict the fate of solvents and optimize the operation of a large scale secondary drying process.

MATERIALS AND METHODS

Compound Selection

The material used in this study was an amorphous spray dried dispersion consisting of 90.9 wt% BMS-817399, a developmental BCS class II chemokine receptor-1 antagonist (Bristol-Myers Squibb, USA) referred to here as Compound A, and 9.1 wt% PVP K30 (Ashland Inc., Covington, KY, USA) (9, 10). Details of the second SDD system including HPMCAS, methanol, acetone and benzene can be found in a separate paper by Yue *et al.* (7).

SEM

The samples were sputter coated using a JFC-1300 auto fine coater (Jeol Inc, MA, USA) and then imaged using a Neoscope JCM-500 (Jeol Inc, MA, USA).

Cryogenic SEM

A cross-section of SDD sample mounted in Tissue-Tek® O.C.T.™ (Sakura Finetek Europe B.V., The Netherlands) was imaged using a Hitachi S-4700 field emission scanning electron microscope (Hitachi, Maidenhead, UK) equipment with a cryogenic chamber (Gatan Inc., Abingdon, UK). The details of this sample preparation and the results can be found in (9).

PXRD

Powder X-Ray Diffraction data were collected using a Bruker-AXS D8 Discover with GADDS system. The x-ray generator was operated at 40 kV and 40 mA with a Cu target (CuKα λ=1.5418 Å), Göbel mirror optics with a 0.5 mm snout collimator, and Hi-Star Detector set at 175 mm sample-detector distance. Integration was set at 3–33 °2θ with a data collection time of 300–1200 s. Data were analyzed using MDI Jade 9.

DSC

DSC data was collected on a PerkinElmer 8500 (HyperDSC®) under a 20 mL/min N_2 purge and Heating rate of 50°C/min.

Vapor Sorption Chamber

A microprocessor-controlled vacuum oven (VWR Model 1430 M) was modified and converted to a sorption chamber. This chamber is equipped with a load cell (Sartorius WZA523-CW) and connected to a mass spectrometer (Ametek ProMaxion Dry[i]), as shown in Fig. 2. 20 to 30 g of wet SDD product is placed in the suspended weighing pan in the chamber and weight loss is automatically recorded at the set temperature and vacuum level. In the course of drying, the vapor phase composition is also monitored by MS. The drying process is over when the weight curve reaches a plateau and does not change any more with time. The dried sample is then analysed by using gas chromatography (GC), PXRD, and DSC.

There is no temperature sensor to monitor the surface temperature of the SDD sample but instead it is assumed that the particle temperature is the same as the oven temperature in this study.

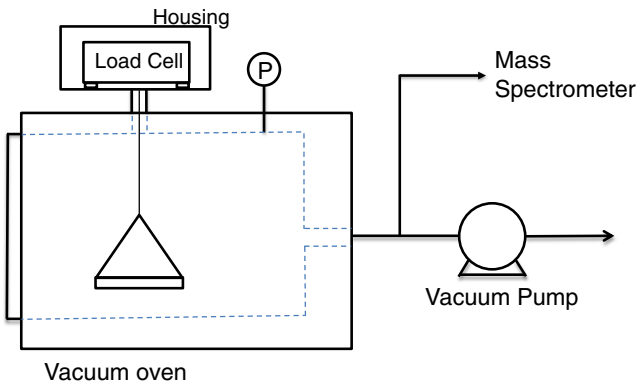

Fig. 2 Schematic diagram of the sorption chamber.

PSD

Particle size distribution was determined as a dry dispersion using a Malvern Morphologi G3 particle characterization system (Malvern Instruments, Malvern, UK). The details of this PSD method are provided by Gamble *et al.* (9).

GC Method

An Agilent Model 6890 GC equipped with a split/splitless injector, a flame ionization detector (FID) and an Empower data acquisition system was used for GC separation and detection. The method was performed on a capillary column with 5% diphenyl and 95% dimethyl polysiloxane stationary phase (30 m×0.32 mm×1.5 µm, Restek). The injector temperature was set at 165°C and the detector temperature was set at 280°C. The GC oven temperature was held at 40°C for 1 min, then programmed to 55°C at a rate of 5°C/min, further increased to 225°C at a rate of 40°C/min, and then held at 225°C for 6 min. Helium was used as the carrier gas at a constant flow rate of 1.8 mL/min. A split flow of 60 mL/min was used. Standard solution (0.2 µL/mL) and SDD sample solution (50 mg/mL) were prepared using dimethyl sulfoxide (DMSO) as the solvent. 1 µL of the solution were injected by an Agilent Model 7683 autosampler. The method has a linear range 0.04 to 2 µL/mL of methanol in DMSO. The percentages of relative standard deviation (%RSD) of methanol peak area response were within 5% for 6 injections of standard solution at two levels (0.04 and 0.2 µL/mL). Percent recoveries at three spiked concentration levels (0.04, 0.2, and 2.0 µL/mL) ranged from 98 to 104%.

Modelling of Secondary Drying in SDD Product

The mathematical equation of non-steady state diffusion in a flat slab (11), as shown in Fig. 3, is set up to describe the removal of organic solvent from wet SDD product. The justification of using a slab is discussed in the "Results and Discussion" section. By assuming a constant diffusion coefficient (D), one-dimensional diffusion and no reaction, this non-steady state diffusion equation, can be written as follows:

$$D\frac{\partial^2 C}{\partial \mathcal{Z}^2} = \frac{\partial C}{\partial t} \tag{1}$$

Initial Condition:

$$C = C_0,\ t = 0,\ -l < \mathcal{Z} < l$$

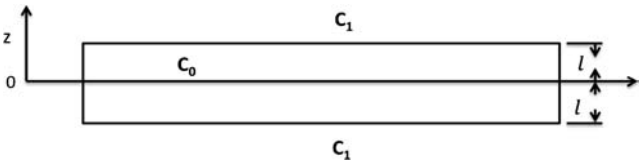

Fig. 3 Geometry of the slab and the schematic of drying process.

Boundary Conditions:

1. $\mathcal{Z} = l,\ C_1 = 0,\ t > 0$

2. $\mathcal{Z} = -l,\ C_1 = 0,\ t > 0$

where D is the diffusion coefficient, C is the concentration of solvent, $\mathcal{Z}$ is the axis of the diffusion, t is time, C_0 is the initial concentration of organic solvent in wet SDD before the secondary drying and C_1 is the concentration of solvent at the surface of the slab. The thickness of the flat slab is 2 l. The selection of the thickness of the slab as 2 l makes the solving of Eq. (1) easier because the concentration profile in the slab becomes symmetrical and the flux of the diffusion is zero as Z is equal to zero. A uniform solvent concentration at the beginning of the drying C_0 is assumed.

The partial differential Eq. (1) can be solved by separation of variables and its solution is available in literature (11–13). The solution of Eq. (1) in terms of concentration as a function of time and location can be integrated through the sheet from $-l$ to $+l$ to provide the measurable quantity in terms of the fraction of solvent remaining in the slab as a function of drying time as follows:

$$\frac{M_t}{M_0} = \sum_{n=0}^{\infty} \frac{8}{(2n+1)^2\pi^2} \exp\left\{-\frac{D(2n+1)^2\pi^2 t}{4l^2}\right\} \tag{2}$$

where M_0 is the weight of solvent in the wet SDD product before the secondary drying, M_t is the weight of solvent in the SDD product at drying time t, and n is an integer. The ratio of M_t to M_o means the fraction of solvent remaining in the wet SDD product. At the beginning of the diffusion when time is equal to zero, the value of M_t to M_o is 1 and when the solvent is completely removed from the wet SDD product, the ratio is equal to 0.

Although Eq. (2) provides the relationship between the weight change and drying time, the series in this equation converges very slowly with time and it does not offer a short and clear analytical relationship between the weight change and the drying time at the beginning of the diffusion process, when t is small. This kind of relationship can be obtained from the solution of Eq. (1) via the Laplace transformation, as described in literature (11–13). After the elimination of terms when the time is small, the solution from the Laplace transformation can be reduced to following expression:

$$\frac{M_t}{M_0} = 1 - 2\left(\frac{D}{\pi l^2}\right)^{1/2} (t)^{1/2} \tag{3}$$

It should be noted that Eqs. (2) with infinite terms and (3) with only two terms yield the same result when the value of time is small, which is demonstrated in the "Result and Discussion" section. Equation (3) offers two useful features of the Fickian diffusion (11–13). First, the plot of dimensionless M_t/M_0 *vs.* the square root of drying time, $(t)^{0.5}$, is linear when time is small. This linear relationship is also valid when the value of M_t/M_0 is less than or equal to 0.5 for Fickian diffusion (12). Second, the value of the diffusion coefficient D can be determined from Eq. (3) if the diffusion length 2 l is known.

Equation (2) shows that the dimensionless M_t/M_0 is a function of drying time t and two parameters, D and l. The term l is half of the diffusion length. In this study, these two parameters D and l are combined as one parameter β and this parameter is called the diffusion parameter and is defined as follows:

$$\beta = \frac{D\pi^2}{4l^2} \tag{4}$$

With the definition of β, Eq. (2) can be re-written as follows:

$$\frac{M_t}{M_0} = \sum_{n=0}^{\infty} \frac{8}{(2n+1)^2\pi^2} \exp\left\{-(2n+1)^2 t\beta\right\} \tag{5}$$

Equation (5) provides a very useful relationship between the dimensionless M_t/M_0 and the drying time t with one parameter β. As defined in Eq. (4), both the diffusion length and the diffusion coefficient are included in β. At the same value of M_t/M_0, as the diffusion length increases, the value for β decreases and the drying time will increase; as the value for the diffusion coefficient increases, the value for β increases and consequently the drying time will decrease.

When there are two kinds of solvents A and B in a wet SDD drug product, the relative diffusion rate of solvent A with respect to solvent B can be defined as follows:

$$\propto_{AB} = \frac{\beta_A}{\beta_B} = \frac{D_A\, l_B^2}{D_B l_A^2} = \frac{D_A}{D_B} \tag{6}$$

Since both solvents A and B have the same diffusion length, $l_A = l_B$, the relative diffusion rate α_{AB} is simply the ratio of the

diffusion coefficient of solvent A to the diffusion coefficient of solvent B. When the value of α_{AB} is equal to 1, both solvent A and solvent B will diffuse out of the shell at the same rate. If the value of α_{AB} is higher than 1, solvent A will diffuse out of the shell faster than solvent B.

RESULTS AND DISCUSSION

Secondary Drying of Wet SDD of Compound A and PVP K30

The SEM images (Fig. 4a to c) clearly demonstrate that the SDD particle morphology is consistent with that of hollow, spherical particles. Some broken pieces are also present as shown in Fig. 4c. The cryogenic SEM imaging as shown in Fig. 4d enabled measurement of individual particle diameters and wall thicknesses (Fig. 5) across the particle size range of 10 to 100 μm (shown in Fig. 6). The measured data (Fig. 7) demonstrated that the wall thickness measurements from representative particles, ranged from approximately 1.5 to 6.9 μm, increasing with particle diameter (14 to 49 μm), with the percentage ratio of particle wall thickness to particle diameter typically between 10 and 15% across the measured size range.

Ideally spherical coordinates should be used for the diffusion equation. However, the curvature effect can be neglected for a hollow sphere if the ratio of the inner radius to the outer radius is close to one. In our case, this ratio ranges from 0.7 to 0.8 (Fig. 7 shows wall thickness is 10 to 15% of the diameter) and hence, rectangular coordinates of a slab are used for the derivation of the diffusion equation as shown in Fig. 3.

PXRD experiments showed that the SDD material contains no residual crystalline phase. DSC experiments also confirmed that the SDD material is a single amorphous phase. Only a single glass transition temperature (T_g) value is observed (onset = 124.17°C, Tg Half Extrapolated = 127.59°C), demonstrating a uniform phase in the bulk (Fig. 8).

The wet SDD product with 90.9 wt% API (Compound A) and 9.1 wt% PVP K30 was prepared by Bend Research in a laboratory scale spray dryer (GEA Pharma PSD1). The vapor phase composition during drying of this wet SDD in the sorption chamber at 50°C and 20 mmHg was monitored via Mass Spectroscopy (MS).

Figure 9 shows that the weight loss changes quickly at the beginning and then gradually slows down. Finally, there is no more weight loss after 800 min of drying time. The total weight loss on drying is 6.53 wt%. The GC results showed that the dried product contained less than 0.3 wt% of methanol.

The results from MS, as shown in Fig. 10, indicate that the MS intensity of methanol increases rapidly at the beginning of drying, but levels off after 700 min which is in a good agreement with the results of LOD *vs.* time shown in Fig. 9

Figure 9 shows the weight loss is proportional to time at the beginning of drying (0–5 min) which may be attributed to the evaporation of solvent from surface of SDD particles, controlled by the constant heat transfer rate from the surrounding environment to the particles. After the initial linear behavior in Fig. 9, the rate of weight loss becomes slower, indicating

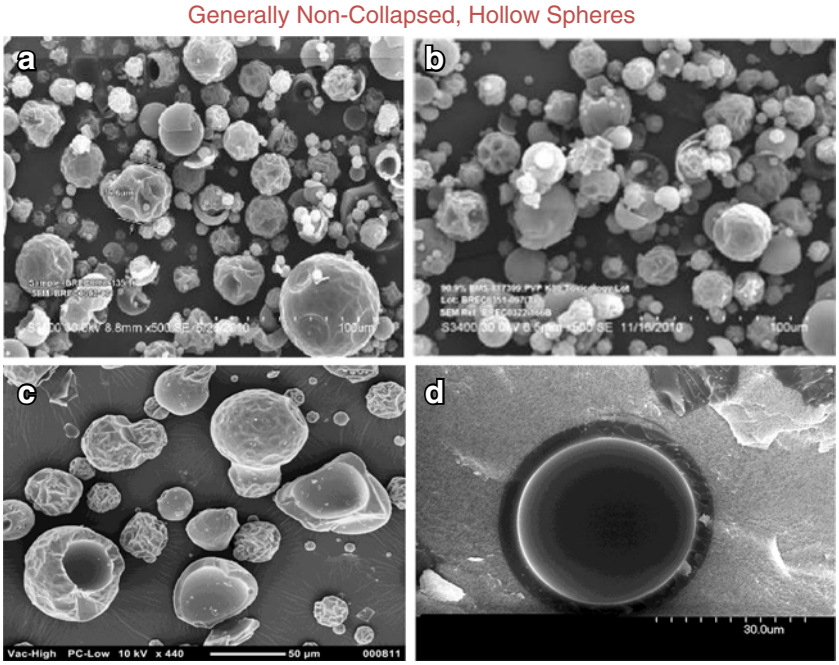

Fig. 4 SEM image of SDD particles of Compound A/PVP K30.

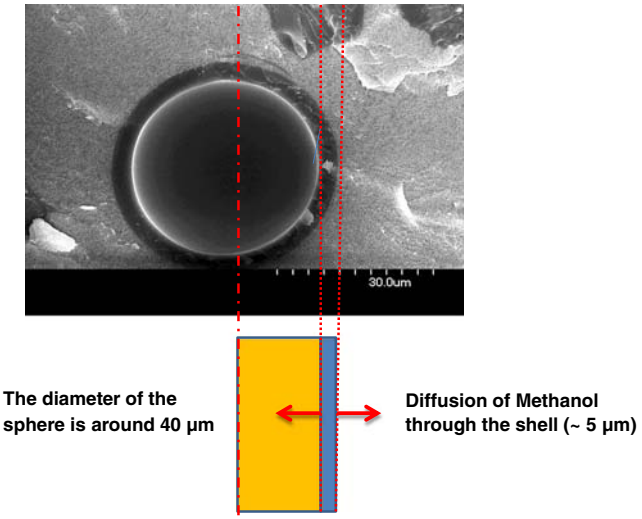

Fig. 5 Schematic diagram of methanol removal from SDD drug product.

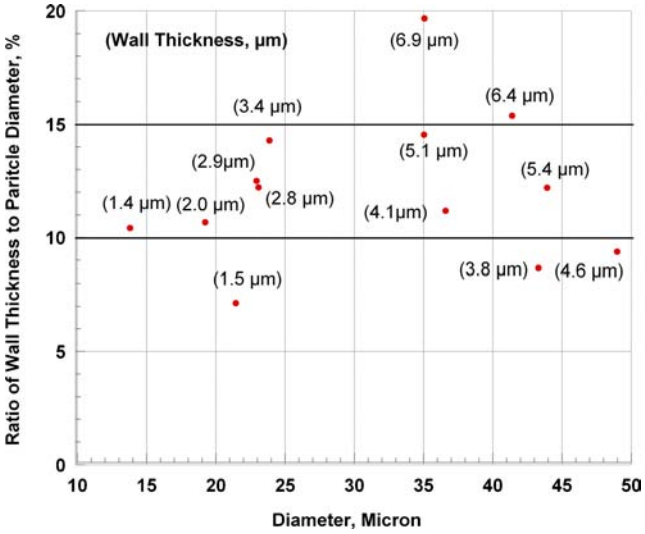

Fig. 7 Ratio of wall thickness to particle diameter.

that the drying mechanism changes from evaporation to a different mechanism.

To elucidate the drying mechanism after the surface evaporation period, the weight loss of methanol from wet SDD is plotted against square root of time [$(\text{time})^{0.5}$] in Fig. 11 as per Eq. (3). The linear behavior as shown in Fig. 11 is attributed to the diffusion of methanol from the wall of the SDD particle (Fig. 5). It should be noted that the weight of the wet cake levels off after the value of the $(\text{time})^{0.5}$ is higher than 30 $(\text{minute})^{0.5}$, (900 min), as shown in Fig. 11. The value of the weight at 900 min is 23.4 g which is the weight of the dried cake. Then the difference between the weight at the beginning of the diffusion 24.8 g and at the end of the drying 23.4 g is the amount of methanol at the beginning of the diffusion process, 1.4 g. This is the value for M_0 defined in Eqs. (2), (3) and (5). This calculation also shows that the methanol concentration before the start of the diffusion process is 5.6 wt% (1.4 g/24.8 g) which is important for the determination of the glass transition temperature of the wet SDD product. As shown in Fig. 11, this linear behavior is valid from the beginning of the diffusion until half of the total amount of methanol in the wet SDD is removed which is equal to $0.5M_0$. Such linear behavior is classified as Fickian diffusion as described in the literature (12) and also can be determined from the solution of Eq. (1) as expressed by Eqs. (2) and (3) in the "Materials and Methods" section.

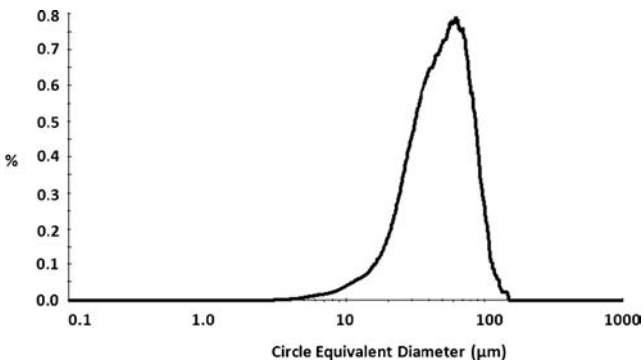

Fig. 6 Particle size distribution of SDD particles of Compound A/PVP K30.

It is noted that there is no anomalous behavior in the profile (Fig. 11) suggestive of molecular relaxation and changes in the rubbery/glassy state of the SDD that are influencing the diffusion process. This finding is supported by the glass transition temperature of the wet product (methanol and Compound A/PVP K30) as a function of methanol concentration, which was measured in a separate experiment using DSC and is shown in Table I.

Knowing the glass transition temperature at various solvent concentrations tells us explicitly whether the material is in a glassy or rubbery state during drying. Since the methanol concentration in the wet Compound A/PVP K30 is 5.6 wt%, the glass transition temperature of the wet SDD will be well above the drying temperature of 50°C based on the Table I. To provide further confidence, the glass transition temperature of this wet SDD can be calculated by using the Fox equation as reported by Sperling (14) because the concentration and the glass transition temperature of methanol (5.6 wt% and $T_g = -169.3$°C (15)) and Compound A/PVP K30 (94.4 wt% and $T_g = 127.59$°C (Fig. 8)) are known. The result of this calculation gives a glass transition temperature of 72°C for the wet SDD. Since the drying temperature is 50°C, which is at least 10°C below the glass transition temperature determined through either approach, the diffusion process occurs in the glassy state from the beginning to the end of the drying.

The focus of this study is on the understanding and the modeling of diffusion of methanol through the shell since this mechanism represents the major mass transfer resistance for

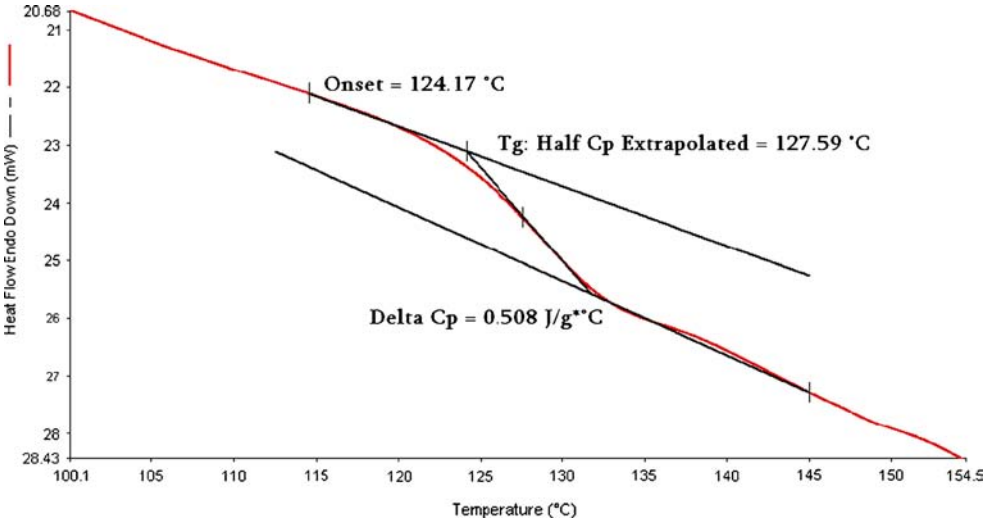

Fig. 8 Glass transition temperature of dried SDD of Compound A/PVP K30.

methanol removal. Therefore, two adjustments on data, as shown in Fig. 11, are made for the establishment of the modeling for this diffusion process. First, the start of the diffusion process follows the end of the evaporation process which lasts for 10 min and hence, the diffusion process starts at t_0 which is set at 10 min after the beginning of the drying process. Second, the amount of the methanol removed via evaporation is subtracted out from the total amount of methanol removal by calculating the difference between cake weight at drying completion (23.4 g at 900 min) and start of the diffusion process (24.8 g at 10 min); hence the value for M_0 is 1.4 g. After these two adjustments, M_t/M_0 is plotted *vs.* $(\text{time})^{0.5}$, as shown in Fig. 12.

In Fig 12, M_t/M_0 plotted *vs.* $(\text{time})^{0.5}$ shows a linear relationship between the value of M_t/M_0 and $(\text{time})^{0.5}$ until the value of M_t/M_0 is slightly over 0.5. This linear behavior of Fickian diffusion as shown in Fig. 12 can be used to determine the value of the diffusion parameter β. Two steps are involved in this determination. First, the slope of the linear relationship between M_t/M_0 and $(\text{time})^{0.5}$ as shown in Fig. 12 is used to determine the value of D/l^2 from Eq. (3). Second, after the value for D/l^2 is known, the value of the diffusion parameter β can be calculated from Eq. (4) and its value is 0.02. It should be noted that the particle size of SDD product varies as shown in Figs. 4 and 6 and accordingly the thickness of the shell is not uniform (Fig. 7). Hence, the value for β of each particle varies and as such the value of β obtained from Fig. 12 is a lumped diffusion parameter.

After the value of the diffusion parameter β is calculated from Eq. (4), the relationship between M_t/M_0 and $(\text{time})^{0.5}$ can be determined from Eq. (5). It is interesting to note that Eq. (5) has an infinite number of terms. However, the contribution to the value of M_t/M_0 becomes insignificant after the

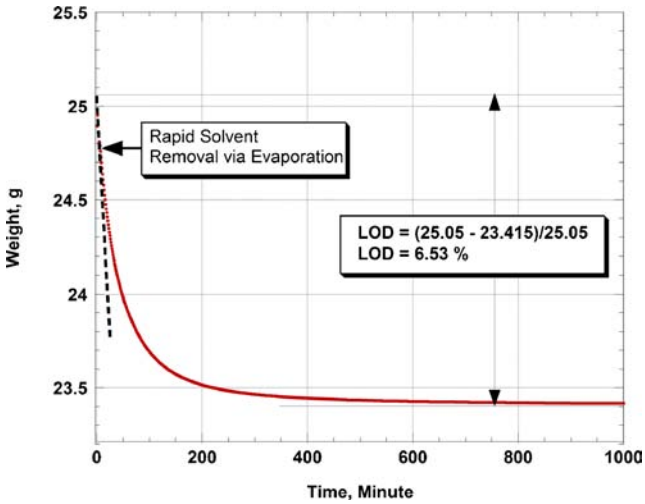

Fig. 9 Drying curve of SDD of Compound A/PVP K30 at 50°C and 20 mmHg.

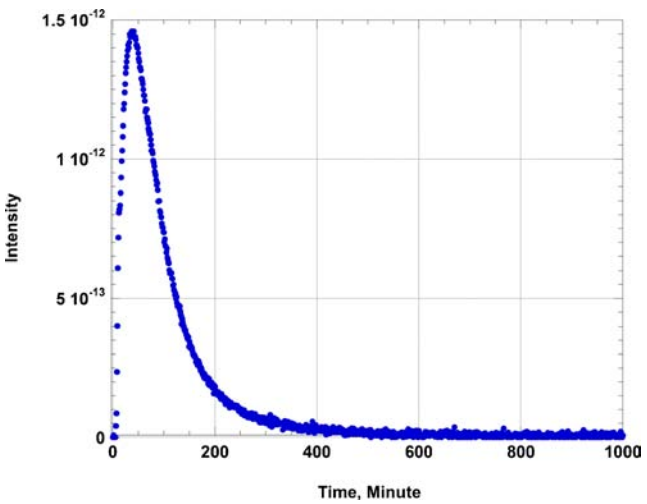

Fig. 10 Methanol vapor phase composition during drying of SDD of Compound A/PVP K30 at 50°C and 20 mmHg.

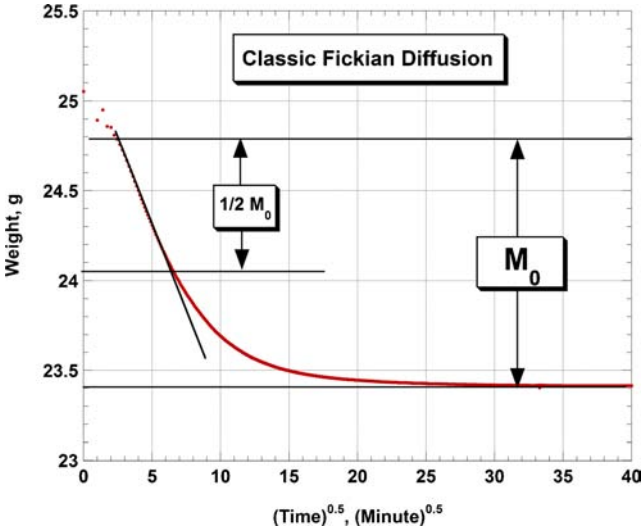

Fig. 11 Diffusion of methanol from SDD of Compound A/PVP K30 at 50°C and 20 mmHg.

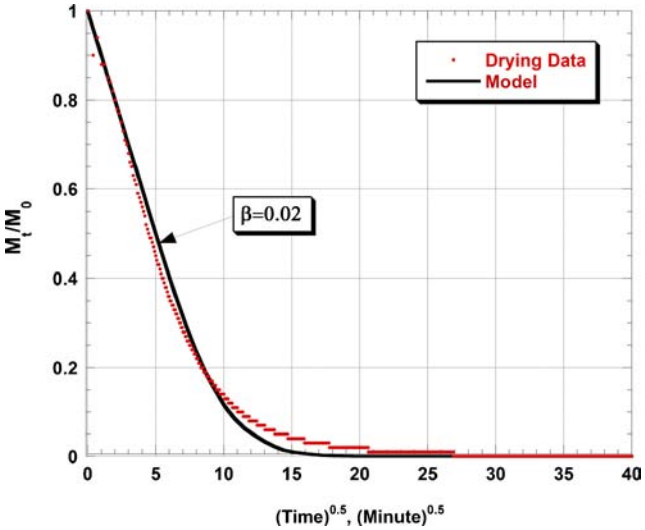

Fig. 12 Comparison of drying data at 50°C and 20 mmHg with the diffusion model.

value of n is greater than 20. Hence, any term with the number higher than 20 can be truncated.

The experimental data of M_t/M_0 *vs.* $(\text{time})^{0.5}$ are in excellent agreement with the prediction from Eq. (5) with $\beta = 0.02$, for the value of M_t/M_0 from 1 to 0.15, as shown in Fig. 12. However, some discrepancy between the data and the prediction is noticed when the value of M_t/M_0 is less than 0.15. This means that it takes longer than predicted from the model to remove the residual solvent when the fraction of solvent remaining in SDD particles is lower than 0.15. The acceptable level of methanol in dried product in this study is 1%. This level translates to a Mt/M_0 ratio of 0.17, which is located in the region where an excellent agreement between the model and the experimental data is demonstrated. Thus the model established in this study can be used to capture the key physical aspects of the complex drying process although it slightly under predicts the residual solvent concentration profile.

Another limitation of the model is that the effect of solvent on the diffusion coefficient is not very conclusive. The dependence of the diffusion coefficient on solvent concentration for polymer solvent systems has been extensively discussed in literature (11, 12, 16) and is normally studied in well-defined polymer geometry where the diffusion length is known. In this study, due to the particle size distribution, the diffusion length is combined with the diffusion coefficient in one lumped parameter β defined in Eq. (4). However, an estimated diffusion coefficient of 8.2×10^{-12} cm^2/sec was calculated from β using an average shell thickness of 4 μm as shown in Fig. 7. This value is typical for the diffusion of gas or vapor in solids and in polymers (17), suggesting the model is valid.

This established model is further verified with the experiments discussed in the subsequent sections: the fate of methanol in SDDs containing Compound A and PVP K30 at different scales with different types of dryers and the fates of methanol, acetone and benzene in HPMCAS SDDs using a tray dryer. The value of the diffusion parameter β in the established model for each case is determined from the fitting of the experimental data.

Table I Glass Transition Temperature of Compound A/PVP K30 and Methanol

Methanol Concentration, wt%	Glass Transition Temperature, °C
2.45	81.4
2.69	76.8
3.73	66.8
4.32	72.2
4.55	64.6
4.62	64.1
6.45	58.0

Scale Up of the Secondary Drying of SDD of Compound A and PVP K30

The secondary drying of SDD of Compound A and PVP K30 was scaled up from a lab scale of 25 g in the temperature-

Table II Operation Conditions and Controlled Parameters from Lab Scale to Kilo Scale

Scale, g	Equipment	Temperature,°C	Tip speed, m/sec	β
25	Oven	50	No agitation	0.02
500	Agitated dryer	60	1	0.035
500	Agitated dryer	60	2	0.035
500	Agitated dryer	40	2	0.013
500	Tray oven	40	No agitation	0.013

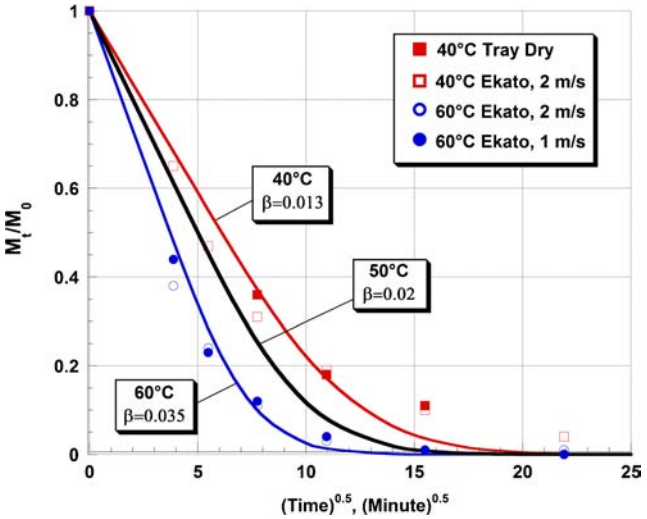

Fig. 13 Scale-up of secondary drying at various temperatures.

controlled sorption chamber to a bench scale of 500 g in a 3-liter Ekato agitated helical conical dryer or in a large tray oven. The agitated operating conditions in terms of drying temperature and tip speed are summarized in Table II. The results of the removal of methanol in terms of M_t/M_0 *vs.* $(\text{time})^{0.5}$ are presented in Fig. 13. Particle size data (not shown) indicated there was no evidence of particle attrition during secondary drying.

Figure 13 shows the drying performance at 60°C is almost identical at two tip speeds (1 and 2 m/sec) suggesting the removal of methanol from the SDD shell is independent of the tip speed. This is because the major mass transfer resistance of methanol diffusion through the shell is temperature dependent; hence, the Fickian diffusion model with the β value of 0.035 is sufficient to describe the drying performance at two different tip speeds as shown in Fig. 13. A very good agreement is obtained between the experimental drying data at 60°C and the drying performance from the Fickian diffusion model over the entire concentration range.

The drying at 40°C was conducted in an agitated dryer at 2 m/sec and in a large tray oven. The drying performance in the agitated dryer exhibits a faster methanol removal than that in the large tray oven until 100 min [$(\text{time})^{0.5} = 10$]; However, after 100 min of drying time, these two exhibit similar drying performance. It is not clear why there is some discrepancy in methanol removal rate between these dryers. One of the possible reasons for this discrepancy is due to the poor heat transfer in the large tray oven at the beginning of drying. The Fickian diffusion model with the β value of 0.013 is used to describe the drying performance at 40°C.

Once the effect of temperature on the removal of the solvent from SDD system is studied and understood in a bench scale setup as shown in Fig. 2, the diffusion model can be established as illustrated in this study and the process can be scaled up to a commercial size secondary dryer.

The Fate of Organic Solvents in Placebo HPMCAS SDD

HPMCAS, one of the most commonly used polymers for SDD (1), was utilized to study the fate of methanol, acetone and benzene (a potential impurity in the input spray solvent) during the secondary drying. The details of experimental conditions (*e.g.* material, preparation, drying conditions, analytical methods) can be found in the study conducted by Yue *et al.* (7). Since the concentration of benzene in input solvent could be very low, (*e.g.* at or lower than a few ppm), 200 ppm benzene was spiked into the polymer solution prepared for spray-drying (4% HPMCAS, 96% methanol or acetone) to give detectable concentrations throughout the course of secondary drying and allow elucidation of the diffusion of benzene in SDD product.

In the course of the drying, the residual concentrations of benzene and methanol or acetone in the SDD were analyzed periodically by GC. The results of these analyses are listed in Tables III and IV.

Table III Benzene and Methanol Concentrations in SDDs Sprayed from Methanol Before and During the Course of Secondary-Drying using a Tray Dryer at 40°C/15%RH

Drying time (hour)	Square root of drying time (min)	M_t^b - Benzene concentration in total SDD (ppm, w/w)	M_t/M_0 (benzene)	M_t^b - Methanol concentration in total SDD (ppm, w/w)	M_t/M_0 (methanol)
0	0.0	5.6(M_0^a)	1.000	17,748 (M_0^a)	1.00000
1	7.7	4.0	0.714	4511	0.25417
2	11.0	2.8	0.500	1340	0.07550
4	15.5	1.4	0.250	105	0.00592
8	21.9	0.5	0.089	6	0.00034
16	31.0	undetectable	0.000	4	0.00023
24	37.9	undetectable	0.000	4	0.00023

[a] M_0 concentration of solvent in total SDD before secondary-drying (i.e. wet SDD)

[b] M_t concentration of solvent in total SDD at each time point of secondary drying

Table IV Benzene and Acetone Concentrations in SDDs Sprayed From Acetone Before and During the Course of Secondary-Drying using a Tray Dryer at 40°C/15%RH

Drying time (hour)	Square root of drying time (min)	M_t[b] - Benzene concentration in total SDD (ppm, w/w)	M_t/M_0 (benzene)	M_t[b] - Acetone concentration in total SDD (ppm, w/w)	M_t/M_0 (acetone)
0	0.0	6.3 (M_0[a])	1.000	27,384 (M_0[a])	1.00000
1	7.7	4.6	0.730	11,533	0.42116
2	11.0	2.7	0.429	3459	0.12631
4	15.5	1.2	0.190	445	0.01625
8	21.9	< 0.5	0.063	23	0.00084
16	31.0	Undetectable	0.000	1	0.00004
24	37.9	Undetectable	0.000	1	0.00004

[a] M_0 concentration of solvent in total SDD before secondary-drying (i.e. wet SDD)

[b] M_t concentration of solvent in total SDD at each time point of secondary drying

The concept of the dimensionless weight loss *vs.* $(\text{time})^{0.5}$ from Eq. (5) is applied to the methanol system and the acetone system and the results are presented in Figs. 14 and 15, respectively. The drying performance for all solvents can be described well by using the diffusion parameter β and Eq. (5), further verifying the model with a different polymer and solvent system. For the methanol system, the value of the diffusion parameter β for methanol and benzene is 0.02 and 0.004, respectively, and the diffusion rate (α_{AB}) relative to benzene is 5 (Table V).

For the acetone system, the value of diffusion parameter β for acetone and for benzene is 0.016 and 0.006, respectively, and the relative diffusion rate (α_{AB}) is 2.7 (Table VI).

The different value of β for benzene in the acetone system (0.006) compared to methanol system (0.004) may be attributed to differences in the shell thickness. The particle size from acetone-HPMCAS SDD system with $D_{90}=26$ μm is much smaller than that from methanol-HPMCAS SDD system with $D_{90}=69$ μm; consequently, the shell thickness from acetone-HPMCAS system is thinner, resulting in a larger value of β.

It was noted that, as expected and shown in Table VII below, the relative diffusion rate (α) for the three solvents followed the same ranking as predicted by solvent transport properties such as kinetic diameter (available in literature (18, 19)) and molar volume (calculated from density and moelcular weight of solvent).

Diffusion of Solvent in SDD Systems

The glass transition temperature (T_g) of the polymer and solvent mixture is a very important index to classify the diffusion behavior (16). If the diffusion occurs at the temperature above T_g, the polymer is in a rubbery state and some theory can be applied to predict the diffusion behavior. However, if the diffusion occurs at the temperature below T_g, the polymer is in a glassy state which is not in an equilibrium state and some anomalous behavior may be expected.

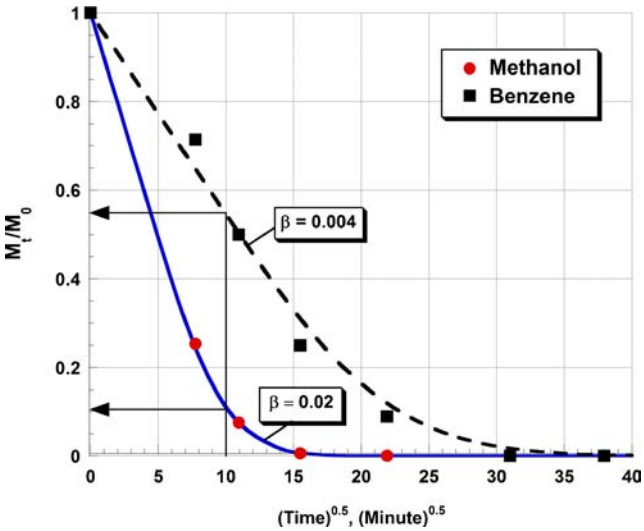

Fig. 14 Removal of methanol and benzene from SDD of HPMCAS at 40°C/15%RH.

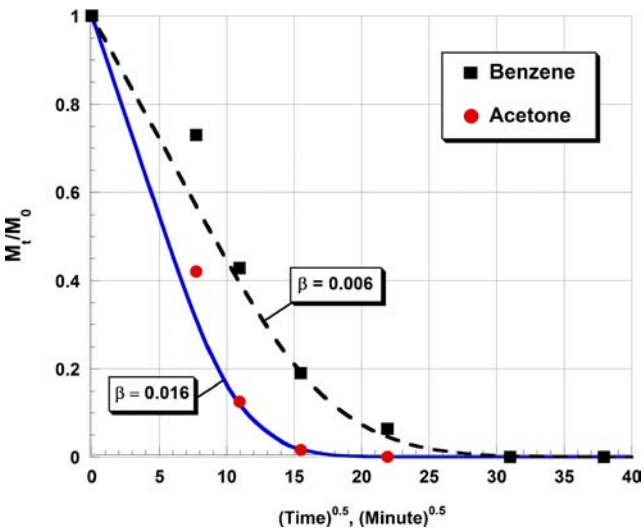

Fig. 15 Removal of acetone and benzene from SDD of HPMCAS at 40°C/15%RH.

Table V Relative Diffusion Rate of Methanol with Respect to Benzene

Solvent	Name	Diffusion parameter, β	α_{AB}
A	Methanol	0.02	5
B	Benzene	0.004	1

The glass transition temperature of polymer and solvent can be measured by using DSC or calculated by using Fox equation if the glass transition temperatures of polymer and solvent as well as the composition of the polymer and solvent mixture are known. The glass transition temperatures of the solvent free solids are provided in Table VIII.

The glass transition temperature of the wet product (methanol and Compound A/PVP K30) was discussed previously (Table I). The glass transition temperatures of methanol/HPMCAS and acetone/HPMCAS mixture (the glass transition temperature of acetone is assumed to equal to 80% of the absolute melting temperature which gives a T_g value of 142.4 K) were calculated by using the Fox equation and the results are presented in Table IX. The glass transition temperature for both mixtures is around 100°C.

The drying temperatures in this study are at less or equal to 60°C, which is below the glass transition temperatures of the two SDD systems (Tables I and IX). Hence, the drying processes occur in the glassy state. Interestingly, the expected anomalous behavior of diffusion coupled with molecular relaxation in these glassy polymers was not observed. The relaxation process occurs because the glassy polymer is usually not at equilibrium, despite the thermodynamic driving force pushing the material to relax to the equilibrium state (16). One of the reasons for not observing this anomalous behavior is likely due to the low concentration of solvent in our SDD systems and hence a less obvious impact from the relaxation behavior on diffusion. Similar Fickian diffusion was observed for the transport of methanol in a glassy polymer of poly(ethylene terephthalate) (PET) at 35°C when the methanol activity is less than 0.3 and the amount of methanol uptake is low (20). A constant value for the diffusion coefficient was used to describe the diffusion of methanol in this PET glassy polymer. Since the glassy polymer is not at equilibrium, the diffusion theories developed for polymer melts (16) are not applicable to describe the molecular migration in the glassy polymer. This is applicable in the case of benzene, which at a concentration less than 7 ppm will have a negligible plasticizing effect on the system. Hence, only a qualitative description of molecular migration of solvent in glassy polymer systems such as those studied here is provided.

Table VI Relative Diffusion Rate of Acetone with Respect to Benzene

Solvent	Name	Diffusion parameter, β	α_{AB}
A	Acetone	0.016	2.7
B	Benzene	0.006	1

Table VII Solvent Properties and Initial Solvent Concentration in HMPCAS SDD System

Solvent	Kinetic diameter, Å	Molar volume, cm^3/mole	Initial concentration, ppm, w/w	α *
Methanol	3.8	40.5	17,748	5
Acetone	4.7	73.4	27,384	2.7
Benzene	5.85	89.1	5.6–6.3	1

* The diffusivity selectivity with respect to benzene

Projection of the Fate of Benzene in SDDs

The model developed here may be used as described below to evaluate the fate of benzene during secondary drying in conjunction with the primary solvent, and thus assist establishing a control strategy for benzene in SDD. Development of the control strategy is described in a separate study by Yue *et al.* (7).

For a known concentration of benzene and spray-drying solvent in initial wet-SDD, the Fickian diffusion models (i.e. β of spraying drying solvent and α) can be used together to determine the secondary drying time required to reach a particular concentration of residual solvent, and then predict the concentration of benzene present at that time. An example is given in Fig. 14 to illustrate such determination and is described as follows: The methanol concentration in the SDD before the secondary drying (M_0) is 17,748 ppm from Table III. If the acceptable concentration of methanol in the dried product (M_t) is 2000 ppm, M_t/M_0 is 0.11. The value of $(\text{time})^{0.5}$ when M_t/M_0 for methanol = 0.11 can be determined from the methnaol diffusion curve (β = 0.02) and is 10. The value of M_t/M_0 for benzene can be determined from the benzene diffusion curve (β = 0.004) at $(\text{time})^{0.5}$ equal to 10 and its value is 0.55. In this example (for an initial benzene concentration of 200 ppm in the input solvent), the benzene

Table VIII Glass Transition Temperatures of Dried Products of the SDD Systems

System	PXRD	T_g, °C
91% of Compound A and 9% of PVP K30	Amorphous	127.59
HPMCAS	N/A	120
PVP K30	N/A	163

Table IX Glass Transition Temperatures of SDD of Solvent and HPMCAS Mixture

SDD System	Composition, wt %	Glass Transition Temperature, °C
Methanol	1.78	−169.3
HPMCAS	98.22	120
Methanol/HPMCAS Mixture	100	101.3
Acetone	2.74	−131
HPMCAS	97.26	120
Acetone/HPMCAS Mixture	100	100

concentration in wet SDD before the secondary drying (M_0) was 5.6 ppm (Table III). Thus the benzene concentration at the drying time of 100 min ($Mt/M_0 = 10$) can be calculated as $M_t/M_0 * M_0$, giving a value of 3.08 ppm (Table X).

The same calculation may be applied to different benzene concentrations in input solvent by assuming the same proportionality between initial benzene concentration in the input methanol and benzene concentration in wet-SDD before the secondary drying. The same approach may also be used to project the fate of benzene in SDD's spray-dried from acetone as the primary solvent.

Development of a Drying Protocol for Secondary Drying

The establishment of the drying protocol in terms of drying temperature, pressure and agitation is based upon the understanding of the drying mechanism. At the selected drying temperature of 50°C, the operating pressure of the dryer must be at least lower than 412 mmHg, the saturated vapor pressure of methanol at 50 °C. Hence, as the methanol diffuses out of the SDD particles and reaches the surface, methanol will vaporize immediately and its surface concentration becomes zero, necessary to satisfy the boundary conditions of Eq. (1). Agitation is necessary for a large scale drying operation to speed up the contact between the particles and the heated wall to make the heat transfer faster.

Since the secondary drying follows Fickian diffusion (Figs. 12, 13, 14 and 15) and the diffusion coefficient is a function of temperature, this means that the drying is dictated by the process temperature. This is because the diffusion process occurs through the shell of the SDD particles and the shell thickness is not related to the scale of the secondary drying process. Therefore when the drying operation is scaled up, excessive agitation is not necessary. It should also be noted that, due to gentle agitation, no shift in particle size was observed in this study for the two batches, operated at the tip speeds of 1 and 2 m/sec. In general, particle attrition was not observed at most secondary drying conditions because the particles are quite robust to secondary drying.

Table X Fate of Organic Solvents in SDD

Solvent	M_0, ppm (Wet SDD)	$(\text{Minute})^{0.5}$	Time, Min	M_t/M_0	Mt, ppm (Dried SDD)
Methanol	17,748	10	100	0.11	2000
Benzene (200 ppm)	5.6	10	100	0.55	3.08
Benzene (10 ppm)	0.28	10	100	0.55	0.2
Benzene (2 ppm)	0.06	10	100	0.55	0.03

CONCLUSIONS

The mechanisms in the secondary drying have been elucidated and they include a rapid evaporation of solvent from the SDD surface followed by a slow Fickian diffusion through the SDD particle shell. Due to the low ratio of the shell thickness to the diameter of the hollow particle, the curvature effect of the sphere can be neglected and the secondary drying process can be described by using the model of the diffusion in a slab. The diffusion process is temperature dependent and thus the key to a successful scale up of the secondary drying is to control the drying temperature. The fate of organic solvents including benzene can be described by the diffusion model and a mathematical relationship has been established to determine the benzene concentration from the fate of methanol and acetone.

ACKNOWLEDGMENTS

The authors are grateful for the Senior Leadership Team and the project team members at Bristol-Myers Squibb Co. for providing support to accomplish this work. The project team members include Kyle Martin, Dr. Neil Mathias, Dr. Balvinder Vig, Lynn DiMemmo, Dr. Steve Wang and Dr. Steven Chan. The technical team members at Bend Research are greatly acknowledged for their generous technical support for secondary drying. Special thanks are given to Mike Ashton at Intertek Pharmaceutical Services (Manchester, UK) for conducting cryogenic scanning electron microscopy.

REFERENCES

1. Paudel A, Worku Z, Meeus J, Guns S, Mooter GV. Manufacturing of solid dispersions of poorly water soluble drugs by spray drying:

formulation and process considerations. Int J Pharm. 2013;453:263–84.
2. Mooter GVD. The use of amorphous solid dispersions: a formulation strategy to overcome poor solubility and dissolution rate. Drug Discov Today: Technol. 2012;9(2):79–85.
3. Ray R. Addressing solubility challenges: using effective technology & problem-solving for delivery solutions. Drug Dev Deliv. 2012;12(6):26–8.
4. Dobry DE, Settell DM, Baumann JM, Ray RJ, Graham LI, Beyerinck RA. A model-based methodology for spray-drying process development. J Pharm Innov. 2009;4:133–42.
5. McCabe WL, Smith JC, Harriott P. Unit Operations of Chemical Engineering. Fifth Edition, McGraw-Hill; 1993; 803.
6. ICH, Impurities: guideline for residue solvents Q3C(R5). ICH; February 2011.
7. Yue H, Nicholson S, Young J, Hsieh D, Ketner R, Hall R. Sackett J, Bank E, Castoro J, Randazzo M. Development of a control strategy for benzene impurity in HPMCAS-stabilized spray-dried dispersion drug products using a science-based and risk-based approach. Unpublished.
8. Matteucci S, Yampolskii Y, Freeman BD, Pinnau I. Transport of gases and vapors in glassy and rubbery polymers. In: Yampolskii Y, Pinnau I, Freeman BD. Editors. Materials science of membranes for gas and vapor separation. John Wiley & Sons, Ltd, 2006
9. Gamble JF, Ferreira AP, DiMemmo L, Martin K, Mathias N, Schild R, *et al.* Application of imaging based tools for the characterisation of hollow spray dried amorphous dispersion particles. Int J Pharm. 2014;465:210–7.
10. Vickery RD, Stefanski KJ, Su C-C, Hageman MJ, Vig BS, Betigeri S.Bioavailable compositions of amorphous piperidinyl compounds. Geneva (Switzerland): World Intellectual Property Organization; 2013 Jan. International Publication Number: WO 2013/013114 A1.
11. Crank J. The Mathematics of Diffusion. 2nd ed. London (England): Claredon Press; 1975.
12. Vrentas JS, Vrentas CM. Diffusion and Mass Transfer. Florida: Taylor & Francis/CRC; 2013.
13. Basmadjian D. The Art of Modeling in Science and Engineering. Chapman & Hall/CRC: Florida; 1999.
14. Sperling LH. Physical polymer science. 3rd ed. New York (USA): Wiley Interscience; 2001.
15. Dounce SM, Mundy J, Dai HL. Crystallization at the glass transition in super-cooled thin film of methanol, J Chem Physics. 200; 126, 191111.
16. Duda JL. Molecular diffusion in polymeric systems. Pure Appl Chem. 1985;57(11):1681–90.
17. Cussler EL. Diffusion, mass transfer in fluid system. 2nd ed. Cambride (UK): Cambrideg University Press; 1997.
18. Flanigan EM *et al.* Silicalite, a new hydrophobic crystalline silica molecular sieve. Nature. 1978;271:512–6.
19. Cosseron AF *et al.* Adsorption of solvent organic compounds in pure silica CHA, *BEA, MFI and STT-type zeolite. Microporous Mesoporous Mater. 2013;173:173147–54.
20. Chandra P, Koros WJ. Sorption and tranport of methanol in poly(-ethylene terephthalate). Polymer. 2009;50:236–44.